Validation of Mainland Water Level Elevation Products From SWOT Satellite

Linpeng Yu, Haowei Zhang, Wei Gong, and Xin Ma

***Abstract*—The surface water and ocean topography (SWOT) satellite, carrying a Ka-band radar interferometer, is designed to detect global hydrological, ecological, and climatic changes through high-precision measurements of water elevation level and to promote the sustainable use and conservation of water resources. The accuracy of water level elevations of inland from SWOT was verified globally in this article by comparing SWOT data with Hydroweb and G-REALM data, so as to better utilize the advanced global remote sensing observation capabilities of SWOT in hydrology. Through spatiotemporal matching validation, this experiment validates the SWOT data by time series within different regions, confirming that SWOT observations have an accuracy of more than 99% for inland lakes and rivers globally in eight geographic subregions. Compared with Hydroweb and G-REALM, SWOT's lake products have mean absolute error of less than 0.5 and 0.3 m, as well as a root mean square error (RMSE) of less than 1.5 and 2 m, respectively. SWOT's data reduce the error in the measurement of the lake by more than 0.1 m compared with the priori data and improves the accuracy by more than 10%. As for river measurements, SWOT's global average measurement error is less than 0.15 m, with an RMSE of less than 1.5 m, providing highly accurate measurements for rivers in most regions of the world. Overall, the product of SWOT can provide high-precision heights of terrestrial water bodies, which is of great significance for small inland water body measurements, global water quantity monitoring, and water circulation research.**

***Index Terms*—Mainland water, remote sensing, surface water and ocean topography (SWOT), water level elevation.**

I. Introduction

ALTHOUGH terrestrial water accounts for only 3.5% of the global water [1], [2], [3], terrestrial water bodies (including but not limited to lake, river, groundwater, reservoirs, and glaciers) have a significant impact on localized industries, agricultural irrigation, the water cycle, and ecosystems at a global scale [4], [5]. Accurate monitoring of global terrestrial water levels is of great significance for the research of meteorological changes, industrial and agricultural development, and ecosystem evolution [6], [7]. Currently, the main global water level monitoring methods are ground-based and satellite-based monitoring [8]. Ground-based monitoring is mainly based on hydrological stations (water level gauges or pressure transducers) and tide gauge observations [9], [10], [11]. Although ground-based monitoring has been continuously enriched in terms of datasets and improved measurement accuracy and timeliness, the number of hydrological stations worldwide has declined sharply since the 1980s, suffering from high cost, insufficient observational coverage, low accuracy, dependence on corrected datasets, and poor stability.

With the continuous development of remote sensing technology, satellites play an important role in the measurement of inland water bodies. LiDAR altimetry satellites have the advantage of high accuracy, and they can form a virtual station at a fixed location and regularly measure lakes, rivers, and other water bodies within their orbit. For example, the Ice, Cloud, and Land Elevation Satellite-2, can accurately measure the elevation of water by emitting and detecting reflected laser [12]. Those virtual stations play an important role in monitoring water elevation level changes, flood events, seasonal fluctuations, and long-term trends [13], [14], [15], [16]. Currently a lot of scholars have carried out water level research based on LiDAR altimetry satellites [17]. By analyzing TOPEx/POSEIDON data over many years, Mercier et al. [18] demonstrated that the temperature rise in the equatorial region of the Indian Ocean affects precipitation and lake levels in Africa. By analyzing ICESat and ICESat-2 satellite data, Zhang et al. [19] and Phan et al. [20] found that the water levels of 111 rivers and 154 lakes on the Tibetan Plateau increased significantly from 2003 to 2009. Coolcy et al. [21] found that the seasonal fluctuations of the reservoirs were four times as large as those of the natural lakes by comparing the natural lakes and artificial reservoirs. Wang et al. [22] analyzed GLAS data and MODIS data and found a relationship between water level and lake area in Danjiangkou Reservoir. Chen et al. [23] observed that the water levels of 340 lakes in China with a water area greater than 10 km^2 exhibited an increase during the period 2016–2019, with an average increase of 0.34 m per year. Xu et al. [24] observed that water levels of global lakes and reservoirs are rising recently. Therefore, altimetry satellites are widely used for water elevation measurements and hydrological analyses globally.

Manuscript received 27 April 2024; revised 3 July 2024; accepted 25 July 2024. Date of publication 30 July 2024; date of current version 8 August 2024. This work was supported in part by the National Natural Science Foundation of China under Grant 42171464, in part by the Key Research and Development Project of Hubei Province under Grant 2022BCA057, in part by "the Fundamental Research Funds for the Central Universities under Grant 2042023kf0216, Grant 2042024kf0034, and Grant 4106-413000028, and in part by Pre-Research Project under Grant D040107. *(Corresponding authors: Haowei Zhang; Xin Ma.)*

Linpeng Yu is with the School of Information Science and Engineering, Shandong University, Qingdao 266237, China (e-mail: 202100120149@mail.sdu.edu.cn).

Haowei Zhang and Wei Gong are with the School of Electronic Information, Wuhan University, Wuhan 473072, China (e-mail: haoweizhang@whu.edu.cn; weigong@whu.edu.cn).

Xin Ma is with the State Key Laboratory of Information Engineering in Surveying, Mapping, and Remote Sensing, Wuhan University, Wuhan 430079, China (e-mail: maxinwhu@whu.edu.cn).

Digital Object Identifier 10.1109/JSTARS.2024.3435363

Although the elevation accuracy is high, LiDAR altimetry satellites only capture information of discontinuous points on the surface, with limited coverage, making it difficult to obtain complete hydrodynamic zones and hydrological parameters. Microwave altimetry satellites can achieve the array detection for land surface, with a wide coverage range, greatly compensating for the shortcomings of laser altimetry. On 15 December 2022, the NASA of the United States of America launched the surface water and ocean topography (SWOT) satellite. SWOT provides two-dimensional continuous monitoring of the elevation of the ocean surface and land water levels by carrying a Ka-band (35.75 GHz frequency or 8.6 mm wavelength) radar interferometer (KaRIn) [25]. Compared with conventional radar altimetry or laser altimetry satellites, SWOT satellites have the advantages of high accuracy (using multipoint observations with a pulse width of two kilometers and 10 cm or less observation error for lakes and rivers), high temporal resolution, high spatial coverage (90% of land waters from 77°S–77°N latitude) and resolution (10–60 m $\times$ 6 m intrinsic pixel size), and a large mapping width (120 km) [26], [27], [28], [29], [30], [31]. The satellite observes at least 90% of the world's rivers and lakes wider than 50–100 m and reservoirs with a surface area larger than 0.01–0.06 km^2 along a 120 km wide belt using a 21-day repeat orbit cycle [32], [33]. The data from the SWOT satellite provide a new way to accurately measure changes in water elevation level in small bodies of water (e.g., lakes, reservoirs) on land. Therefore, the accuracy of SWOT data needs to be validated to better utilize the advantages of SWOT in hydrology.

At present, most studies focus on the validation of SWOT on existing hydrological models and ocean sea level heights, with less validation on the accuracy of water elevation level of inland lakes and rivers [34]. Whether the SWOT data can accurately reflect the elevations of inland water bodies remains to be verified [35]. In this experiment, based on the theory of spatiotemporal matching, Hydroweb and G-REALM product data were used to validate the accuracy of the water elevation levels of the SWOT satellite's lake and river products (Lake V2.0 and River V2.0) [36], [37], [38]. In conclusion, this experiment aims to verify the accuracy of SWOT measurements by evaluating and calculating specific indexes, such as mean error and root mean square error (RMSE) [39]. The results will provide support for monitoring water body elevation and observing the global water circulation.

II. Materials and Methods

A. Satellite Data

This experiment primarily uses SWOT's Lake and river vector dataset. Since SWOT began collecting data, many different datasets have been made available to the public on the NASA website, including those for lakes and ocean surfaces. The SWOT Level 2 Lake Single-Pass Vector Data Product (Version 2.0) and SWOT Level 2 River Single-Pass Vector Data Product (Version 2.0) were used as the primary data sources in this article [40], [41], [42]. This dataset provides water surface elevation, area, storage change derived from the high-rate data stream from the KaRIn. The dataset covers the surface lakes and rivers studied in this experiment, covering an area of 90° north–south latitude and 180° east–west longitude. The dataset contains data from 21 June 2023, to present. Also, due to the SWOT satellite swath width of 120 km, most of the area was observed more than once in a cycle (21 days). The "Lat," "Lon," "wse," and "wse_u" fields in the product were used in this experiment to obtain the elevation and mass marker values corresponding to the water level positions in the SWOT measurements. Among the extracted fields, the "wse" field represents the measured elevation value under the measurement point, and the "wse_u" field is a quality control field.

The data were preprocessed to minimize errors and the impact of anomalous observations on the experiment. Using the mass marker values, data with wse_u $>$ 1 were excluded to remove large values of measurement error and to safeguard the validity of the data. The original SWOT data are retained in the experiment. This is because the datum of the elevation data measured by SWOT is the same as the datum of the validation data adopted subsequently, and the error between the two is small. This data were obtained according to the corresponding link.[1]

B. Surface Lake and River Level Monitoring Data

For a comparison with actual lake and river water elevation level, the G-REALM and Hydroweb data were introduced into the experiments [43], [44]. The G-REALM website utilizes the Topex/Jason series, ENVISAT, and a mix of Interim Geophysical Data Record datasets to provide time series of water elevation level changes in some of the world's largest lakes and reservoirs. The accuracy of the technology and the data on the website have been verified in a variety of aspects, which can reflect the actual state of the lake water elevation level veritably. This experiment extracted the text files of lake status from the website and extracted the water elevation level of the required lakes as the actual values to verify the accuracy of SWOT satellite water elevation level measurement. This data were obtained according to the corresponding link.[2] The Hydroweb website collects hydrological observation data from multiple data providers, including ground stations, remote sensing data, and satellite data [45]. These datasets cover hydrological monitoring information from all over the world. The location and water elevation level data were extracted from the website. This data were obtained according to the corresponding link.[3]

In this experiment, all lakes included in the validation were divided into nine regions—namely, Africa (AF), Europe and Middle East (EU), Siberia (SI), Central and Southeast Asia (AS), Australia and Oceania (AU), South America (SA), North America and the Caribbean (NA), North American Arctic (AR), and Greenland (GR)—by geographical area, as shown in Fig. 1 [46]. The distribution of lakes in the Hydroweb validation set is indicated by the red dots on the map. The distribution of lakes in the G-REALM validation set is indicated by the blue dots.

[1][Online]. Available: https://podaac.jpl.nasa.gov/dataset/SWOT_L2_HR_LakeSP_2.0 and https://podaac.jpl.nasa.gov/dataset/SWOT_L2_HR_RiverSP_2.0, Accessed: Mar. 15, 2024.

[2][Online]. Available: https://ipad.fas.usda.gov/cropexplorer/globaleservoir/, Accessed: Mar. 15, 2024.

[3][Online]. Available: https://hydroweb.theia-land.fr/, Accessed: Mar. 15, 2024.

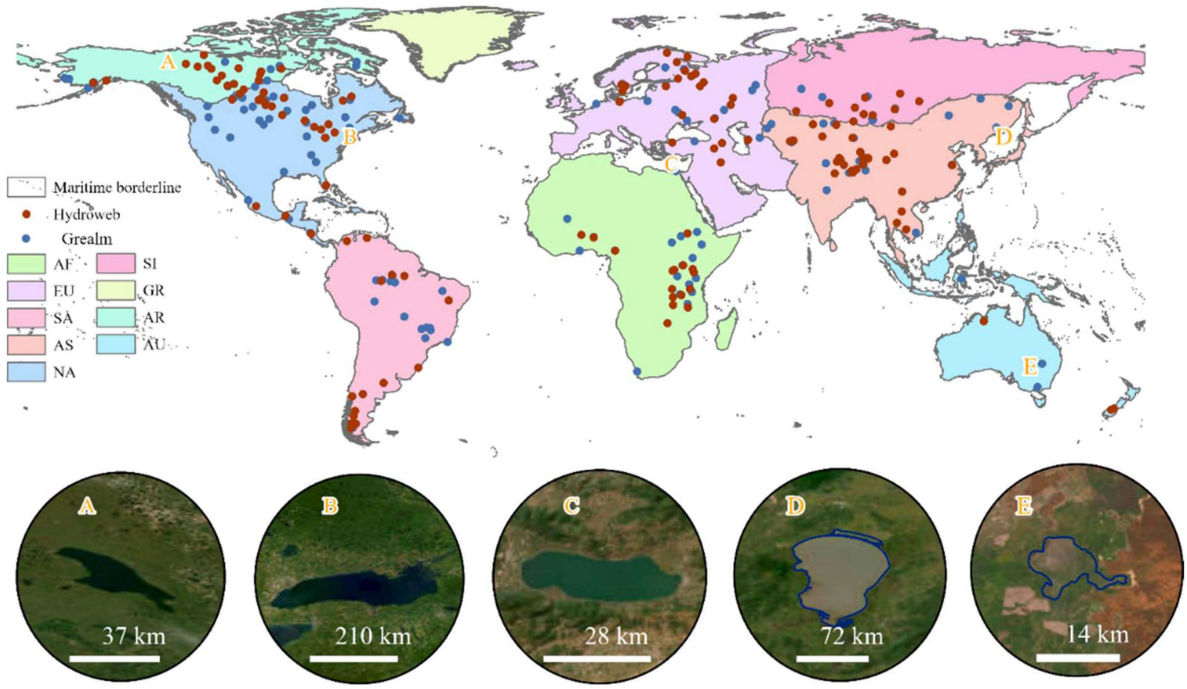

Fig. 1. Geographical distribution of SWOT versus Hydroweb and G-REALM.

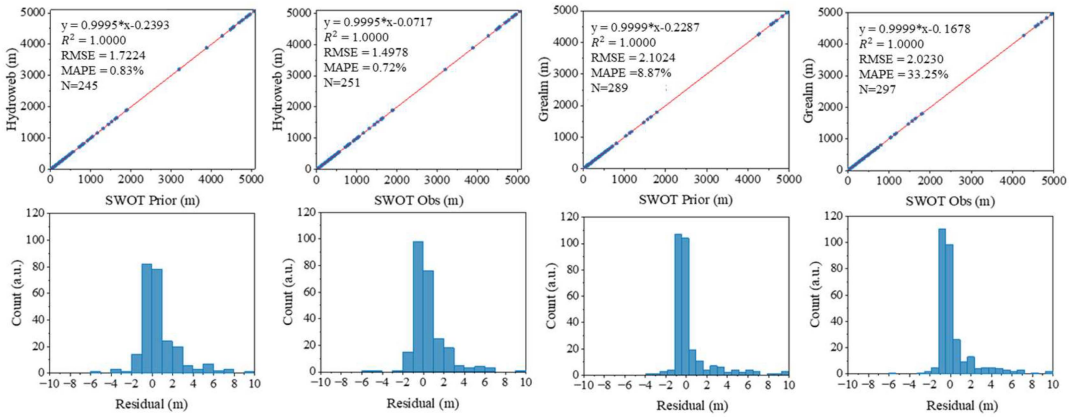

Fig. 2. Relevance of SWOT versus Hydroweb or G-REALM in global lakes.

Hydroweb and G-REALM data were used to perform SWOT accuracy assessment for global regions. In Fig. 1, Mahoney Lake(A), Ontario Lake(B), Kremenchuk reservoir(C), Khanka Lake(D), and Narran Lake(E) were selected to display the time series of lake water elevation levels. A, B, and C were used to show lake level changes over time as measured by Hydroweb and SWOT. D and E were used to show lake level changes over time as measured by G-REALM and SWOT.

C. Methods

Spatiotemporal matching theory was utilized for data validation to evaluate the accuracy of river and lake water elevation levels from the SWOT product. The time interval was 1 day. Spatial matching of the lake products was performed by matching the Hydroweb and G-REALM data with the vector boundaries of the SWOT lake products. The spatial matching of the river products was based on the river width of the virtual sites recorded in the Hydroweb dataset to be used as the diameter of the match, which matched the SWOT river virtual site with the Hydroweb virtual site. The field of "wse" given in the SWOT product is reported with respect to the provided model of the geoid (H_{geoid}) and after using models to accounts for the effects of tides. Specifically, if H represents the geocentric height of the water surface with respect to the reference ellipsoid after corrections for media delays and tidal effects (STide, LTidef, and PTide) were applied, then wse is computed as follows. Therefore, the elevation datum of SWOT and G-REALM and Hydroweb is EGM2008

$$\text{wse} = H - H_{\text{geoid}} - \text{STide} - \text{LTidef} - \text{PTide}. \quad (1)$$

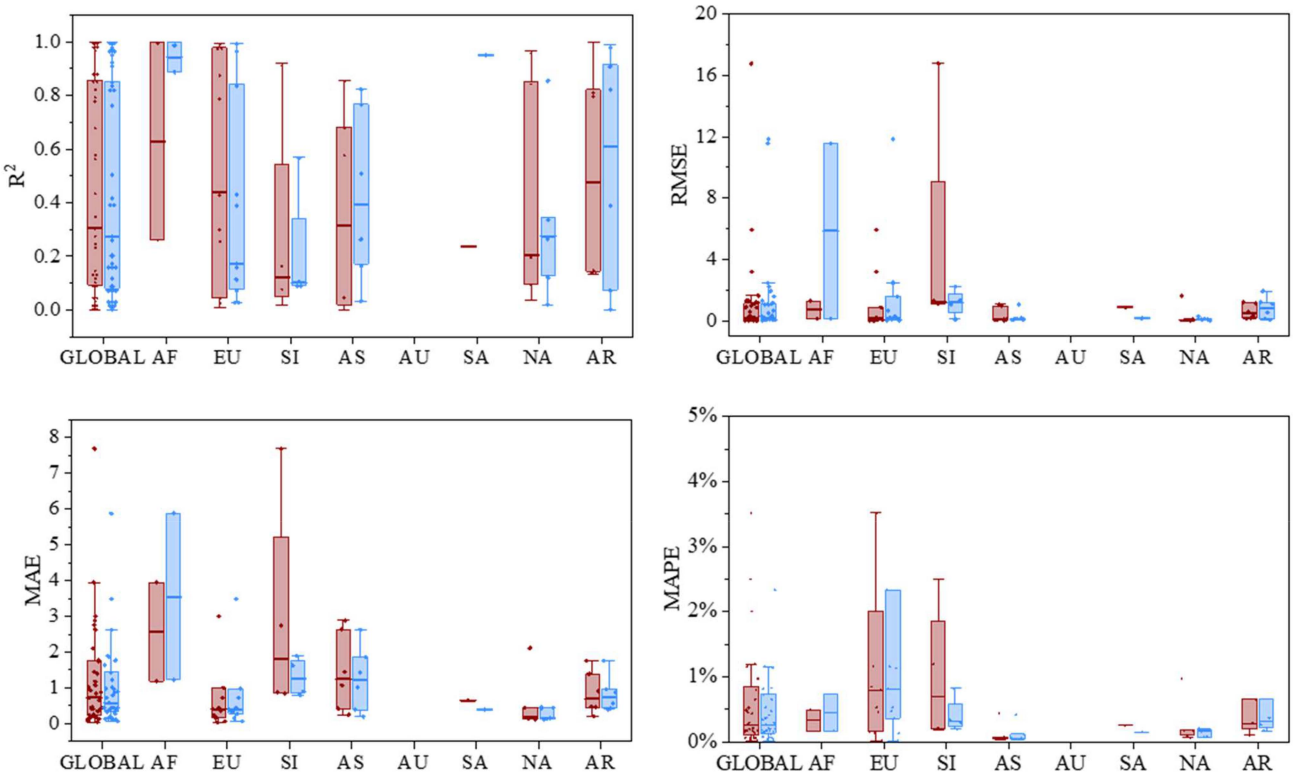

Fig. 3. Box plot of evaluation results for SWOT versus Hydroweb.

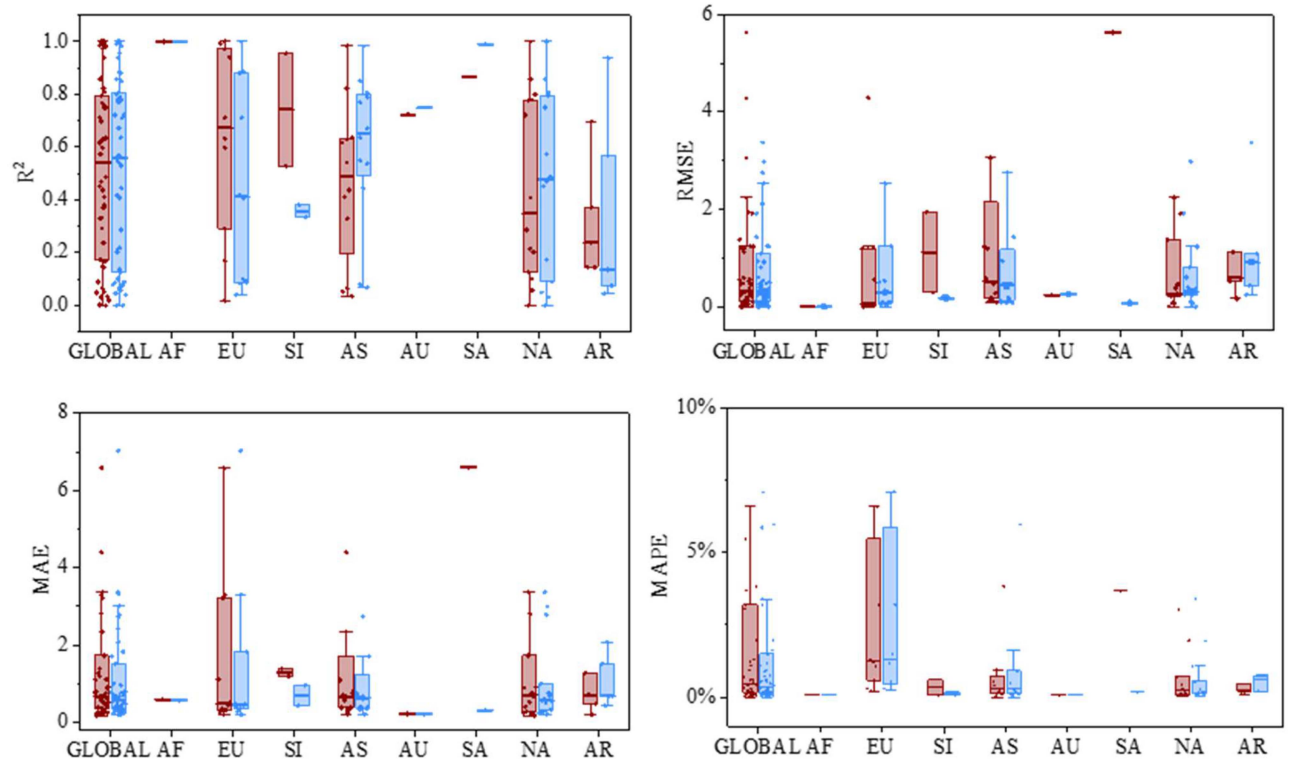

Fig. 4. Box plot of evaluation results for SWOT versus G-REALM.

Least squares fit was employed globally to evaluate the accuracy of SWOT's lake and river products with the G-REALM and Hydroweb. A box-line chat was used to show the distribution of the evaluation indicators [coefficient of determination (R^2), RMSE, mean absolute error (MAE), and mean absolute percentage error (MAPE)] for lakes and rivers globally and in different regions [47]. The box-line chat showed the center of the data, the scatter range, outliers, and fluctuations. Finally, we used histograms to show the distribution of the residuals of the observed and true values for lakes and rivers, which allowed us to determine the bias and tail weight of the residual data.

The product data from SWOT satellite data were used as test data in this experiment. The water elevation levels of lakes and rivers from G-REALM and Hydroweb were used as validation data. The accuracy of SWOT water elevation level was verified according to the following steps.

1) Data were extracted from the validation sets (G-REALM and Hydroweb) based on location information provided by the SWOT product vector data.
2) The SWOT measured water elevation level was matched with the validation datasets provided from G-REALM and Hydroweb, utilizing a 1-day time matching window. The spatial matching of the river used the river width as the search diameter. The spatial matching is achieved using the width of the river and the vector boundary of the lake, respectively. Accuracy assessments were conducted globally and on eight continents.
3) The water level elevation of SWOT lakes or rivers globally and on eight continents was evaluated with the corresponding indicator indices. More specifically, G-REALM and Hydroweb data were combined to demonstrate the accuracy of the five lakes in a time series.

D. Accuracy Assessment

On the basis of the above steps and the validation data provided by G-REALM and Hydroweb, we evaluated the accuracy of SWOT's lake and river elevation level retrieval. The evaluation metrics include 1) R^2, 2) RMSE, 3) MAE, and 4) MAPE. R^2 measures the correlation between a priori and measured water levels. RMSE measures the consistency between a priori and measured water levels in terms of quantity and the magnitude of the error in the quantitative analysis. MAE measures the average of the absolute values of a priori and measured water levels in terms of quantity. MAPE measures the magnitude of the error between a priori and measured water levels in terms of quantity. These assessments are used to compare accuracy across regions and globally

$$R^2 = 1 - \frac{\sum (X-Y)^2}{\sum \left(Y-\bar{Y}\right)^2}, \tag{2}$$

$$\mathrm{RMSE} = \sqrt{\frac{1}{N} \cdot \sum (X-Y)^2}, \tag{3}$$

$$\mathrm{MAE} = \frac{1}{N} \cdot \sum_{i=1}^{N} |X-Y|, \tag{4}$$

$$\mathrm{MAPE} = \frac{1}{N} \cdot \sum_{i=1}^{N} \left| \frac{X-Y}{Y} \right| \tag{5}$$

where X is the water elevation level retrieved by the SWOT, Y is a reference value based on G-REALM and Hydroweb data, N is the total number of validation points selected in the calculation, and $\bar{Y}$ is the average of the reference values.

III. Results

A. Results of Lake Water Elevation Level Evaluation

The SWOT satellite lake products include three data types: priori, observed, and unassigned. The priori and observed data types were chosen to evaluate the lake. The correlation of the SWOT satellite lake product data with Hydroweb and G-REALM is presented in Fig. 2. The SWOT priori products were matched to the Hydroweb dataset for a total of 121 lakes worldwide, accumulating 245 data points, when the Hydroweb product was used as the validation dataset. The SWOT observation products were matched to the Hydroweb dataset for a total of 124 lakes and accumulated 251 data points. In this case, the RMSE of the priori data is 1.7224 m and the MAPE is 0.83%, while the RMSE of the observed data reaches 1.4978 m and the MAPE reaches 0.72%, which is a decrease of 0.2246 and 0.0011, respectively, compared with the other data. Meanwhile, the MEAN decreases by 0.1844. The above changes indicate that under the Hydroweb dataset, the SWOT observations has a smaller bias and a 13% reduction in the overall error rate.

When the G-REALM product was used as the validation dataset, the SWOT priori products were matched to the G-REALM dataset for a total of 118 lakes, accumulating 289 data points. The SWOT observation products were matched with a total of 119 lakes, resulting in 297 data points. The RMSE of the priori data was 2.1024 m, while the RMSE of the observational data decreased to 2.0230 m, which indicates a decrease of 0.0794. The MEAN value decreases from 0.2838 to 0.2033, and the error size decreases by an average of 0.0805. However, a large gap exists between the priori data and the observational data in terms of the MAPE, and the relative error of the observational data was higher because the priori data were only used as a starting baseline, and its accuracy cannot be fully guaranteed. Therefore, the higher error of the priori data itself affects the value of MAPE in this set of results. The above changes show that the degree of deviation between the SWOT observations and the true values decreases under the G-REALM dataset, with most of the observations differing from the true values by no more than 0.2 m. When the SWOT priori data were fitted to the Hydroweb and G-REALM datasets, the fitting error was smaller for the G-REALM dataset and more of the SWOT priori data came close to the values in this dataset. However, the SWOT observations as a whole fit the Hydroweb values more closely, with fewer points deviating from the Hydroweb values. These fitting results show that SWOT has a higher accuracy with an average measurement error of less than 0.5 m on the priori data. The average measurement error on the observed data was less than 0.3 m, proving that SWOT has good measurement accuracy.

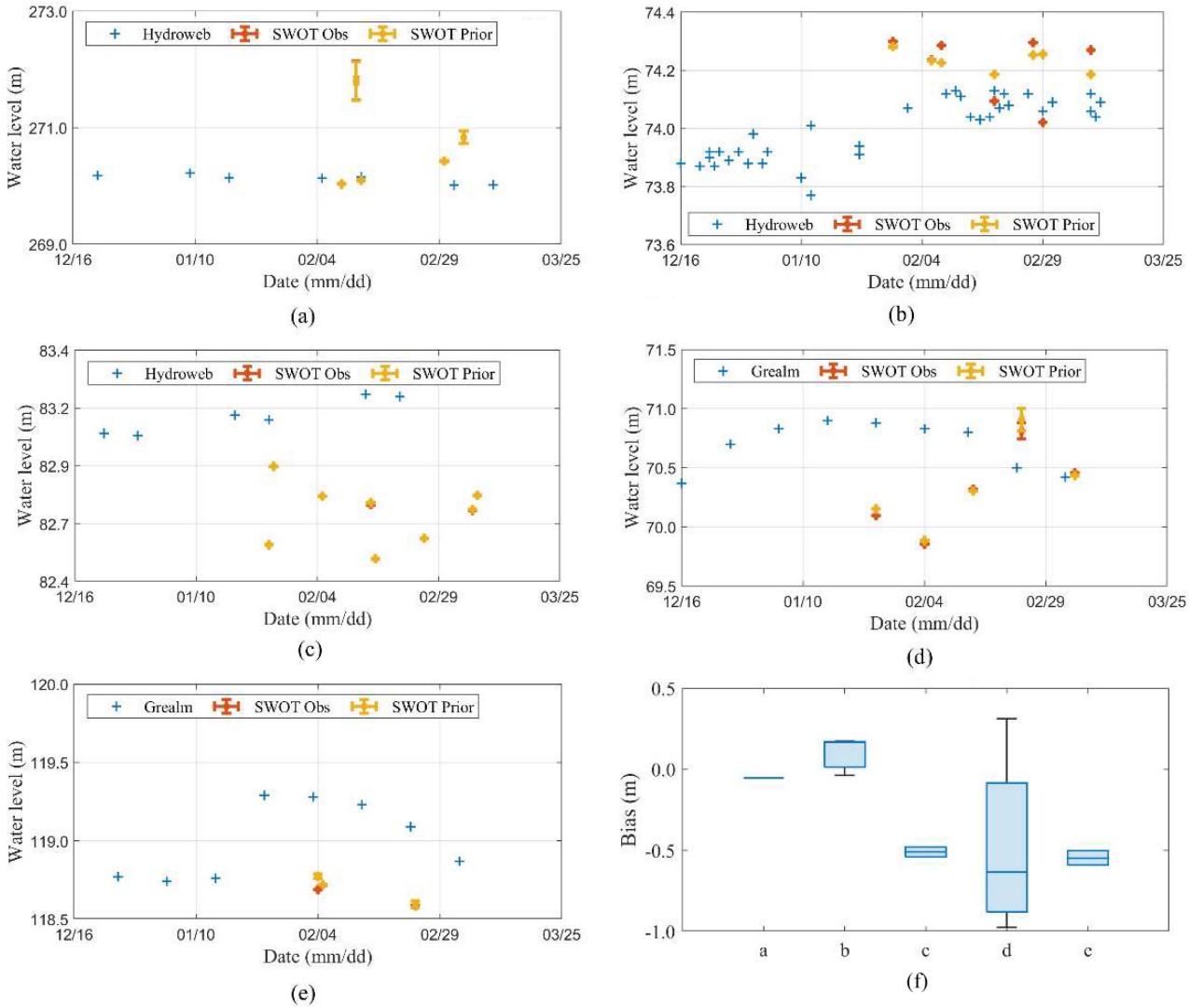

Fig. 5. (a)-(e) represents the time-series distribution of lake elevation levels in Fig. 1(a)-(e). (f) shows the bias distribution of the lake elevations from (a) to (e).

Fig. 3 demonstrates the assessment results of SWOT lake products versus Hydroweb worldwide and in different regions. The red and blue box plots represent SWOT priori and observed data vs. Hydroweb, respectively. The assessment metrics for each lake are shown in the appropriate grouping in Fig. 3 when the number of SWOT versus Hydroweb matches was greater than two. Globally, the R^2 of SWOT's observed product types were similar to the priori product data when compared with Hydroweb. The SWOT observations has a greater R^2 compared with the SWOT priori in the eight regions. In the distribution of RMSE values, the SWOT observations had fewer outlying bad points and the RMSE values were basically the same as the SWOT priori data. However, a deviation occurred in the AF region, which may be due to the limited number of measurement points. The SWOT observations had smaller variance and lower median in MAE and MAPE values, proving that the SWOT observations have smaller errors and error probabilities compared with the priori data. Overall, the SWOT observations data were better than the SWOT priori data in terms of measurement accuracy and degree of bias. The exception is the AF region, where the limitation in the number of measurement points results in larger differences in values. The SWOT observations data improved by 13% on RMSE, 27% on MAE, and 12% on MAPE. The improvement was significant in EU, SI, and SA.

The SWOT observations had slightly larger R^2 values than the priori data on a global scale and in multiple subregions in Fig. 4, indicating a better fit of the SWOT observations to the G-REALM data. The distribution of RMSE values on a global scale showed that the SWOT observations had smaller 75% quantile values compared with the priori data, with most measurement data points having smaller RMSE values. Within specific regions, the RMSE values were significantly lower, except for the AU, AF regional observations, which have the same RMSE values as the priori data. The SWOT measurement dataset had smaller variance and lower median on MAE and MAPE, indicating better precision and error rates compared with the SWOT priori data. However, the SWOT measurements in the AR region were relatively poor in all four metrics, which may

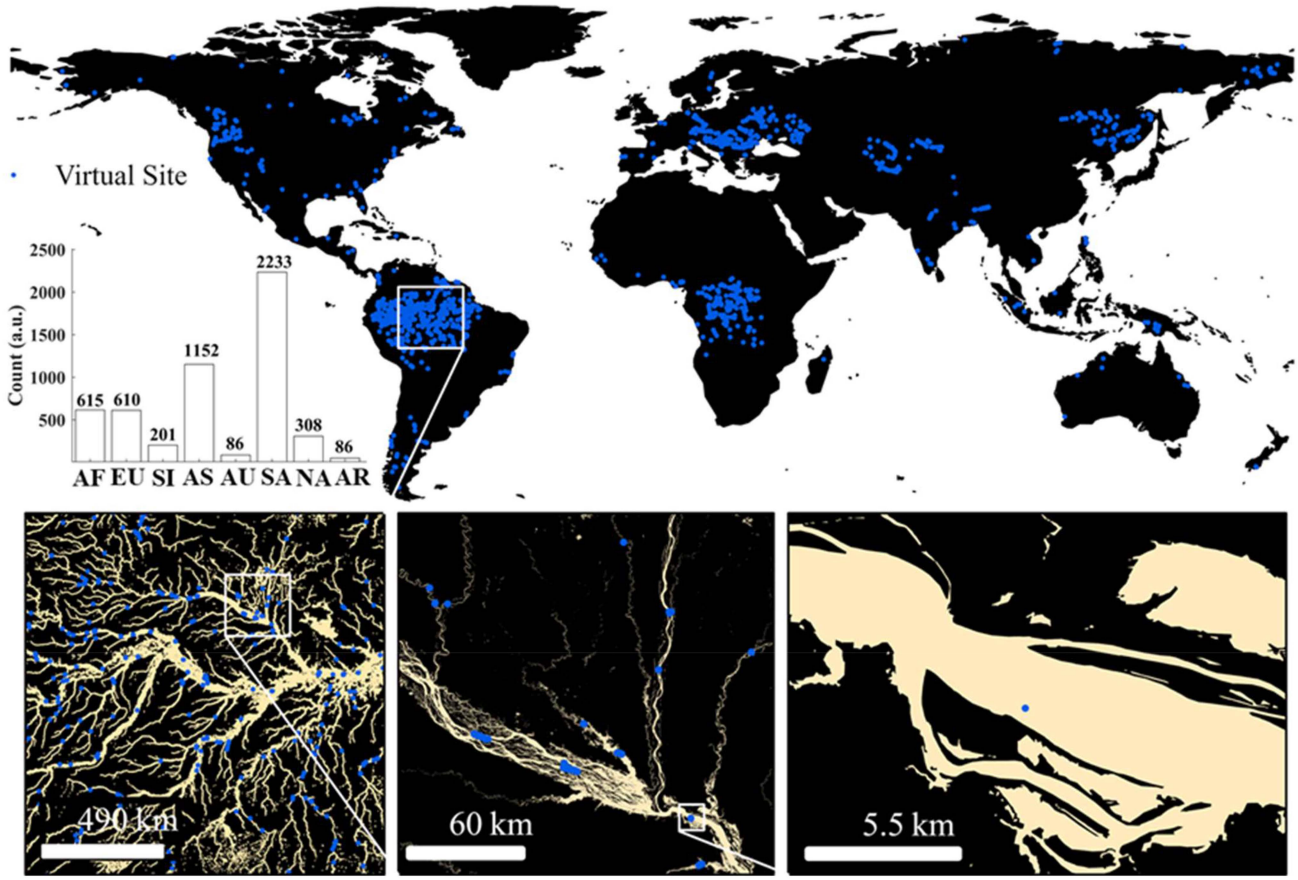

Fig. 6. Distribution of river virtual sites.

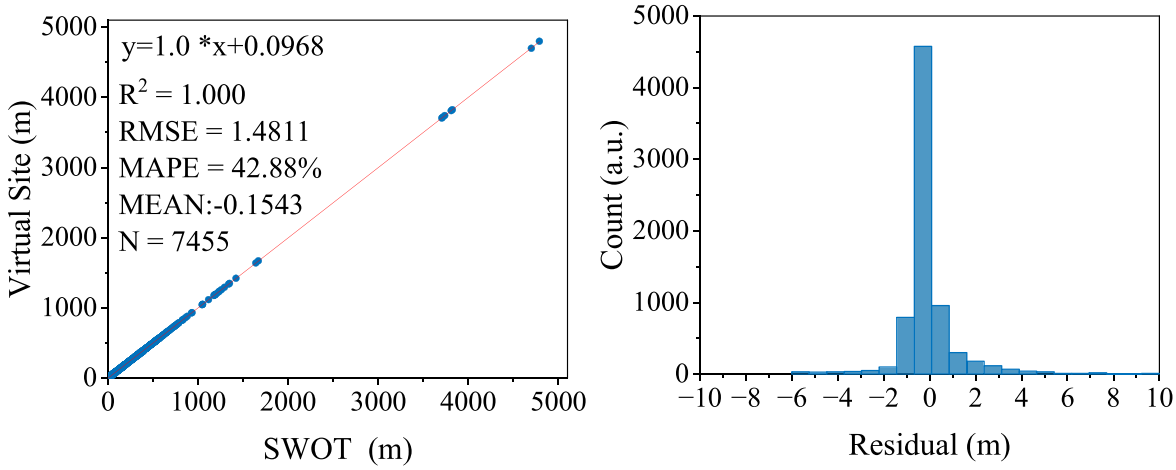

Fig. 7. Global validation results of the river virtual site.

be due to the location of the AR region at high latitudes with few river data and the error of SWOT data for ice observations. Overall, in comparison with the G-REALM data, the SWOT measurements improved by 5% on R^2, 4% on RMSE, 5% on MAE, and 8% on MAPE relative to the priori data. The improvement was significant in the SI, AU, and NA regions.

The time-series distribution of lake water elevation levels from Fig. 1(a) to (e) is displayed in Fig. 5, where the blue data were Hydroweb or G-REALM, respectively. The red and yellow colors that represent the SWOT product data types are observed and priori, respectively. The maximum deviations of individual points in Fig. 5(a)–(e) from Hydroweb or G-REALM were 1.8, 0.2, 0.7, 1.0, and 0.4 m, respectively. The points with the largest deviations in Fig. 5(a) may be caused by errors, with reference to the trend of the Hydroweb data. The R^2, RMSE, and MAE metrics in Fig. 5(a) metrics are poor because only one data point

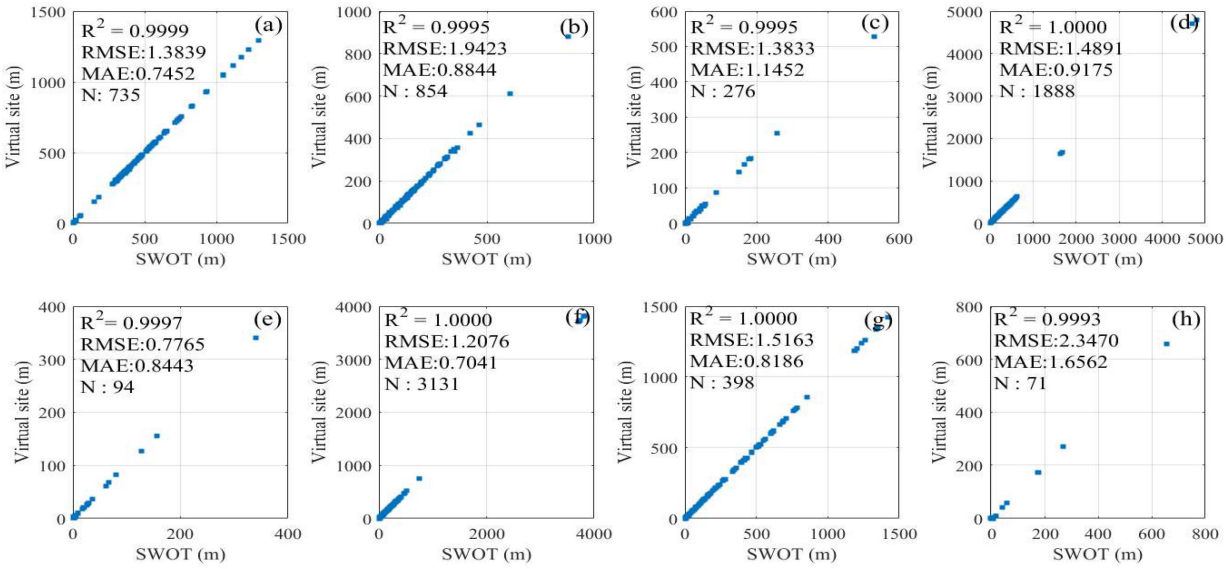

Fig. 8. (a)-(h) represent the results of fitting the SWOT data to the rivers in the eight regions of AF, EU, SI, AS, AU, SA, NA, and AR.

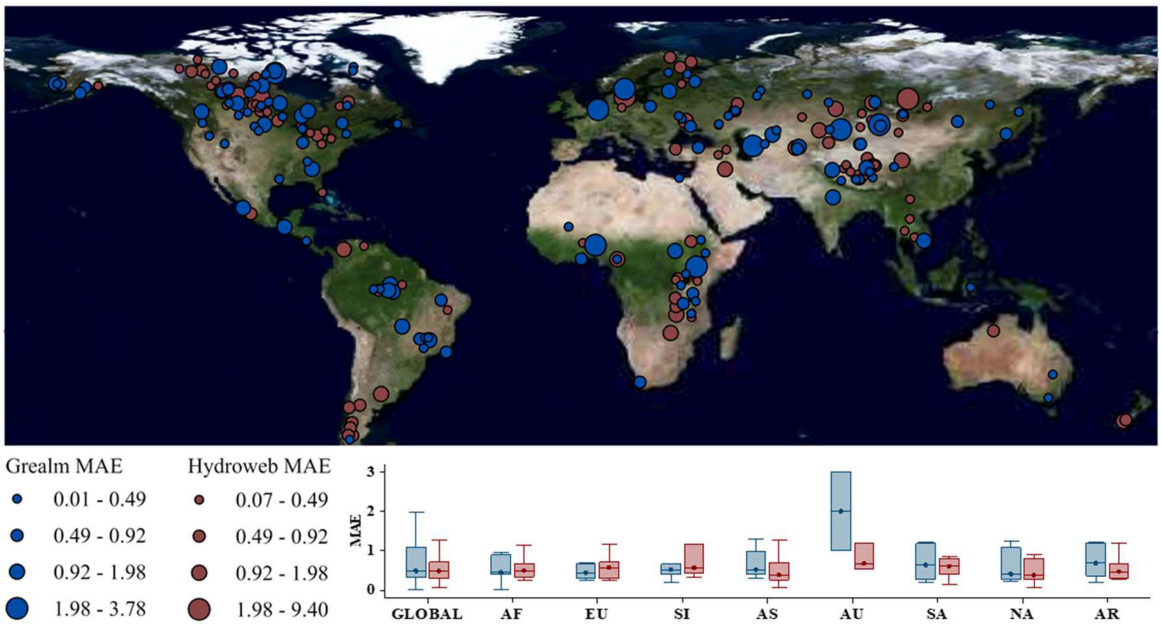

Fig. 9. Distribution of MAE for SWOT lake products vs. G-REALM and Hydroweb.

out of all the data is time aligned. In Fig. 5(b), the R^2 value of the observed data increased compared with the priori data, while the ME and MAE decreased. This finding indicates that the SWOT observed data for this lake can better fit the real data with less error. For Fig. 5(c), the priori data of SWOT and the measured data have the same indexes, such as RMSE, MAE, and R^2, indicating no significant difference in accuracy. However, the priori data of SWOT have a more dispersed distribution of values and a larger standard deviation, which proves that the observed data are closer to the real values. For Fig. 5(d), the MAE of SWOT measured data decreases relative to the priori data, which proves that the error of observed data is smaller. However, the observed data are not as effective as the priori data in terms of the degree of R^2. In addition, the standard deviation of both datasets is larger, and the data are more dispersed possibly because of the change in the lake elevation level during the selected time period. For Fig. 5(e), the error of SWOT measurement data is more obviously higher than the error of priori data, and the observation is less effective. This condition may be due to the fact that the measurement data had fewer sampling points in the selected time interval than the priori data, thereby increasing the error. Overall, the SWOT measurement data showed slightly

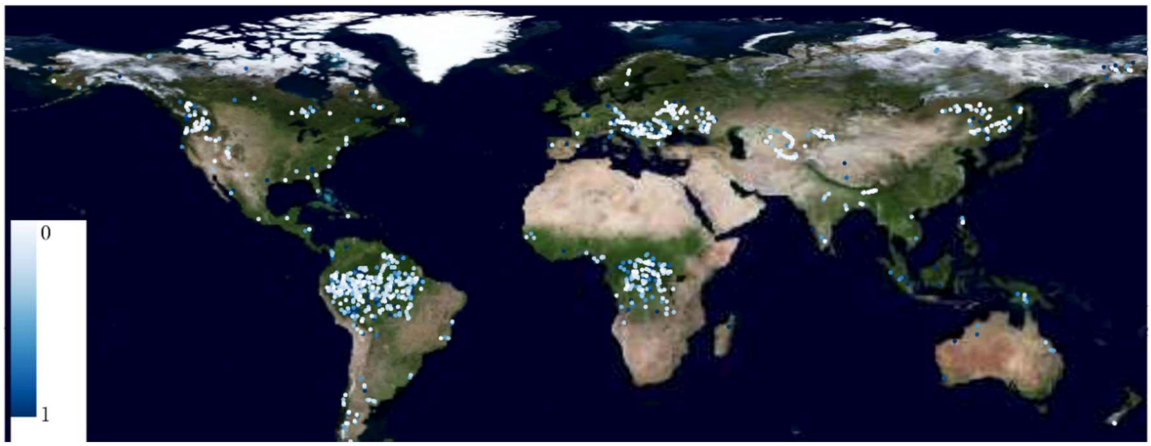

Fig. 10. Distribution of MAE for SWOT river products vs. Hydroweb.

better accuracy than the priori data for specific lakes, with a better overall fit and less error.

B. Results of River Water Elevation Level Evaluation

In terms of validation of lake elevation levels, this experiment statistically samples the water levels of rivers in AF, EU, SI, AS, AU, SA, NA, and AR, and compares them with SWOT measurements to validate the accuracy of SWOT's water elevation level measurements for inland water bodies. Fig. 6 shows the distribution and number of river sampling points in the eight regions. The rivers involved in the validation are primarily located in the SA, AS, AF, and EU regions, while the rest of the regions are less selected due to the geographical distribution of the rivers and the limitation of the water elevation level data. The distribution of one sampling site in the SA region is shown in detail in Fig. 6.

To verify the accuracy of SWOT for river level measurement, this experiment fits the SWOT measurement data to the global 7455 virtual station measurement data in Fig. 6 and analyzes the results as shown in Fig. 7. The left figure shows the fitting results of SWOT observation data and virtual station data, while the right figure shows the distribution of the residuals of the two sets of data. As can be seen from the figure, the R^2 of the two fits is 1, indicating a strong correlation between the two sets of data. Meanwhile, the RMSE of the two groups of data is 1.48 m, and the MAPE is 42.88%. The average error is only -0.15 m, and the residuals of most of the measurement points and the real data are controlled between -1 and 1 m. The SWOT measurement error is controlled within 1% of the true data, indicating that the SWOT measurement accuracy can exceed 99% when compared with the true elevation of the measurement points. These results demonstrate that the SWOT has a high level of accuracy for observing rivers in the eight regions of the world.

The SWOT observations were fitted to the regression of the actual data recorded by virtual stations in eight regions in this experiment to further verify the accuracy of SWOT for river hydrological observation. The results are shown in Fig. 8, where the serial numbers (a)–(h) represent the results of fitting the SWOT data to the rivers in the eight regions of AF, EU, SI, AS, AU, SA, NA, and AR. The figure illustrates that the measurement error of SWOT is controlled within 1 m in all regions, with the exception of the AR and SI region. The RMSE value is also controlled within 2 m, indicating a small deviation for the measured SWOT values and a good match between the true and measured values. For the AR region, the distribution of rivers is less and the sampling points are fewer because of its location in a high-latitude area, which leads to larger differences in individual values. Meanwhile, the rivers have ice most of the time because of the lower temperature in the high-latitude region, which leads to an increase in the deviation between the SWOT measured values and the real values. Overall, the measurement error of SWOT for river water elevation level can be controlled within 1 m, and the overall accuracy can reach more than 99% except for the influence of icing and other problems.

The distribution of MAE when comparing SWOT observations with G-REALM and Hydroweb is shown in Fig. 9. The calculation of MAE provides the average of the absolute values of the prediction errors for each SWOT measurement point, which visually represents the size of the gap between the SWOT observations and the true values, and clearly reflects the measurement accuracy of SWOT. The blue circles represent the locations of the SWOT observations compared with G-REALM. The red circles represent the locations of the SWOT observations compared with Hydroweb, and the size of the circles indicates the size of the MAE values. The box plots show the distribution of MAE for the SWOT compared with G-REALM in blue and the distribution of MAE for the SWOT compared with Hydroweb in red. The median MAE is the same for both datasets globally, but the MAE from SWOT has less variance and a more concentrated distribution compared with Hydroweb, which is relatively better in Fig. 9. The SWOT observations have essentially the same median MAE as the two datasets within specific regions, except in the AU region. In the EU, SI region, G-REALM performs slightly better than Hydroweb, whereas in the SA, NA region, Hydroweb outperforms G-REALM. A few measurement points are present in the AU region and large values are found at individual points, resulting in a large gap

between the two box plots. Hydroweb shows better match with SWOT measurements, with a smaller error range and smaller error values.

Fig. 10 shows the distribution of MAE when SWOT's observations of the river are compared with Hydroweb. Each point on the graph represents a SWOT measurement location, with the color of the point indicating the size of the MAE value. Blue points indicate larger MAE values, while white points indicate smaller MAE values. The points with smaller MAE values (points close to white) are mainly located in South America, central Africa, Europe, North American coastal areas, and the western and southeastern parts of Asia, indicating that SWOT has less error and higher accuracy in the measurement of rivers in the above regions. However, more dark-colored points are found on both sides of the equator, and the measured data have a larger MAE. The water level of rivers in this area may fluctuate significantly due to long-term climate influences. In addition, it takes time for SWOT to repeat measurements in the same area, which leads to discrepancies between the measured data and Hydroweb data, resulting in an increase in MAE. In addition to both sides of the equator, the dark-colored points are distributed in the high-latitude regions of Siberia, northern North America, and Oceania. The measured data may reduce the number and accuracy affected by the icing phenomenon in the high-latitude regions. For Oceania, fewer SWOT measurement points resulted in high MAE values for the overall data. Overall, most of the points are white in Fig. 10, proving that the MAE values of the SWOT measurement points mostly remain below 0.5, and the accuracy of the measurements is high for most of the river water bodies.

IV. Discussion and Conclusion

In conclusion, this experiment analyzes and acquires the SWOT dataset for global lake and river elevation level detection by fitting and distribution of residuals. This work proves the accuracy and feasibility of SWOT satellite altimetry for global lake level measurement and provides the possibility of accurately determining the change in the water elevation level of small terrestrial bodies of water (e.g., lakes and reservoirs). The SWOT lake products are controlled within 0.5 m error globally and within 1% MAPE when compared with Hydroweb. In particular, the errors between the SWOT lake product data and Hydroweb data are small within the AF, EU, AS, SA, and NA regions, and both are well fitted. SWOT's observed data decreased by 0.1 m in mean error and more than 0.2 m in RMSE compared with the priori data, with an overall accuracy improvement of more than 10%. When compared with G-REALM, SWOT's lake product has an average error of less than 0.3 m globally, MAPE within 1%, and an accuracy of more than 99%. Specifically, the lake product errors within the AF, AR, EU, SI, and SA regions are less than 0.3 m, with a high accuracy. SWOT's observed data decreased by 0.3 m in mean error, RMSE decreased by more than 0.2 m, and overall accuracy increased by more than 5% compared with the priori data when using G-REALM as the validation set. Overall, the SWOT lake product has an error of less than 0.5 m in global measurements and an accuracy of 99% for water level measurements. The accuracy is even higher especially in AF, EU, NA, and AS regions, and the error can be less than 0.2 m. In terms of river measurement, SWOT's global average measurement error is within 0.15 m, RMSE is less than 1.5 m, and the overall accuracy is more than 99%. In South America, central Africa, Europe, coastal areas of North America, and western and southeastern Asia, the MAE of SWOT river measurements is less than 0.5, and the accuracy of the measurements is further improved compared with the global average. However, for the data collected and analyzed in this experiment, the accuracy of SWOT in measuring the edge of the water body (under the influence of land) remains to be verified. High resolution, wide coverage, global observation capability, three-dimensional measurement capability and high accuracy are the key advantages of the SWOT satellite for water level elevation measurement. These advantages enable SWOT to provide more detailed and accurate water level elevation than traditional satellite altimeters. In contrast, although ICESat-2 satellites have high-precision laser altimetry capabilities, their coverage and application areas are mainly focused on height measurements of polar ice caps and glaciers, with relatively limited monitoring capabilities for global water bodies. Therefore, SWOT has significant advantages in water level elevation of global water bodies, especially rivers, lakes and coastal areas. SWOT satellites will have a wide range of potential applications in hydrological science, environmental monitoring, disaster management, climate change research and ecological protection. These applications will help to better understand and respond to changes in global water resources and the environment, improve the ability to cope with natural disasters.

Acknowledgment

The numerical calculations in this paper have been done on the supercomputing system in the Supercomputing Center of Wuhan University.

References

[1] C. Verpoorter, T. Kutser, and D. A. Seekell, "A global inventory of lakes based on high-resolution satellite imagery," *Geophys. Res. Lett.*, vol. 41, no. 18, pp. 6396–6402, 2014.

[2] T. Zhang, H. Ren, Q. Qin, C. Zhang, and Y. Sun, "Surface water extraction from Landsat 8 OLI imagery using the LBV transformation," *IEEE J. Sel. Topics Appl. Earth Observ. Remote Sens.*, vol. 10, no. 10, pp. 4417–4429, Oct. 2017.

[3] Y. Meng, P. Du, X. Wang, X. Bai, and S. Guo, "Monitoring human-induced surface water disturbance around Taihu Lake since 1984 by time series Landsat images," *IEEE J. Sel. Topics Appl. Earth Observ. Remote Sens.*, vol. 13, pp. 3780–3789, Jun. 2020.

[4] X. Pi, Q. Luo, and L. Feng, "Mapping global lake dynamics reveals the emerging roles of small lakes," *Nature Commun.*, vol. 13, no. 1, 2022, Art. no. 5777.

[5] N. Xu, H. Lu, W. Li, and P. Gong, "Natural lakes dominate global water storage variability," *Sci. Bull.*, vol. 69, pp. 1016–1019, 2024.

[6] Y. Pokhrel et al., "Global terrestrial water storage and drought severity under climate change," *Nature Climate Change*, vol. 11, no. 3, pp. 226–233, 2021.

[7] J. Yi, J. Wei, Q. Li, and O. O. Ayantobo, "Regional characteristics and impact factors of change in terrestrial water storage in Northwestern China from 2002 to 2020," *IEEE J. Sel. Topics Appl. Earth Observ. Remote Sens.*, vol. 16, pp. 386–398, Dec. 2023.

[8] A. H. Zaji, H. Bonakdari, and B. Gharabaghi, "Remote sensing satellite data preparation for simulating and forecasting river discharge," *IEEE Trans. Geosci. Remote Sens.*, vol. 56, no. 6, pp. 3432–3441, Jun. 2018.
[9] O. Munyaneza and U. G. Wali, "Water level monitoring using radar remote sensing data: Application to Lake Kivu, Central Africa," *Phys. Chem. Earth, A B C*, vol. 34, pp. 722–728, Jun. 2009.
[10] J. Liao, L. Gao, and X. Wang, "Numerical simulation and forecasting of water level for Qinghai Lake using multi-altimeter data between 2002 and 2012," *IEEE J. Sel. Topics Appl. Earth Observ. Remote Sens.*, vol. 7, no. 2, pp. 609–622, Feb. 2014.
[11] T. Perumal, M. N. Sulaiman, and C. Y. Leong, "Internet of Things (IoT) enabled water monitoring system," in *Proc. IEEE 4th Glob. Conf. Consum. Electron.*, 2009, pp. 86–87.
[12] L. Song, C. Song, and S. Luo, "Integrating ICESat-2 altimetry and machine learning to estimate the seasonal water level and storage variations of national-scale lakes in China," *Remote Sens. Environ.*, vol. 294, 2023, Art. no. 113657.
[13] C. Q. Song, Q. H. Ye, and X. Cheng, "Shifts in water-level variation of Namco in the central Tibetan Plateau from ICESat and CryoSat-2 altimery and station observations," *Sci. Bull.*, vol. 60, pp. 1287–1297, Jun. 2015.
[14] Z. Zhang, M. Wang, X. Liu, C. Wang, and H. Zhang, "Map and quantify the ground deformation around Salt Lake in Hoh Xil, Qinghai-Tibet Plateau using time-series InSAR from 2006 to 2018," *IEEE J. Sel. Topics Appl. Earth Observ. Remote Sens.*, vol. 14, pp. 858–869, Oct. 2021.
[15] R. Luo, Q. Yuan, L. Yue, and X. Shi, "Monitoring recent lake variations under climate change around the Altai mountains using multimission satellite data," *IEEE J. Sel. Topics Appl. Earth Observ. Remote Sens.*, vol. 14, pp. 1374–1388, 2021.
[16] H. Villadsen, O. B. Andersen, L. Stenseng, K. Nielsen, and P. Knudsen, "CryoSat-2 altimetry for river level monitoring—Evaluation in the Ganges–Brahmaputra River basin," *Remote Sens. Environ.*, vol. 168, pp. 80–89, 2015.
[17] Y. Ma, N. Xu, J. Sun, X. H. Wang, F. Yang, and S. Li, "Estimating water levels and volumes of lakes dated back to the 1980s using Landsat imagery and photon-counting LiDAR datasets," *Remote Sens. Environ.*, vol. 232, 2019, Art. no. 111287.
[18] F. Mercier, A. Cazenave, and C. Maheu, "Interannual lake level fluctuations (1993–1999) inafrica from topex/poseidon: Connections with ocean-atmosphere interactions over the Indian Ocean," *Glob. Planet. Change*, vol. 32, nos. 2/3, pp. 141–163, 2002.
[19] G. Zhang, H. Xie, and S. Kang, "Monitoring lake level changes on the Tibetan plateau using ICESat altimctry data (2003–2009)," *Remote Sens. Environ.*, vol. 115, no. 7, pp. 1733–1742, 2011.
[20] V. H. Phan, R. Lindenbergh, and M. Menenti, "ICESat derived elevation changes of Tibetan lakes between 2003 and 2009," *Int. J. Appl. Earth Observation Geoinf.*, vol. 17, pp. 12–22, 2012.
[21] S. W. Cooley, J. C. Ryan, and L. C. Smith, "Human alteration of global surface water storage variability," *Nature*, vol. 591, pp. 78–81, 2021.
[22] Y. Wang, "Using MODIS images to examine the surface extents and variations derived from the DEM and laser altimeter data in the Danjiangkou Reservoir, China," *Int. J. Remote Sens.*, vol. 29, no. 1, pp. 293–311, 2008.
[23] J. Chen and J. Liao, "Monitoring lake level changes in China using multi-altimeter data (2016–2019)," *J. Hydrol.*, vol. 590, 2020, Art. no. 125544.
[24] N. Xu, Y. Ma, Z. Wei, C. Huang, and G. Li, "Satellite observed recent rising water levels of global lakes and reservoirs," *Environ. Res. Lett.*, vol. 17, no. 7, 2022, Art. no. 074013.
[25] R. Fjortoft, "KaRIn on SWOT: Characteristics of near-Nadir Ka-band interferometric SAR imagery," *IEEE Trans. Geosci. Remote Sens.*, vol. 52, no. 4, pp. 2172–2185, Apr. 2014.
[26] G. H. Allen and T. M. Pavelsky, "Patterns of river width and surface area revealed by satellite-derived North American River Width data set," *Geophys. Res. Lett.*, vol. 42, no. 2, pp. 395–402, 2015.
[27] G. H. Allen and T. M. Pavelsky, "Global extent of rivers and streams," *Science*, vol. 361, no. 6402, pp. 585–588, 2018.
[28] X. Chen, L. Liu, X. Zhang, S. Xie, and L. Lei, "A novel water change tracking algorithm for dynamic mapping of inland water using time-series remote sensing imagery," *IEEE J. Sel. Topics Appl. Earth Observ. Remote Sens.*, vol. 13, pp. 1661–1674, Apr. 2020.
[29] C. Nickles, E. Beighley, Y. Zhao, M. Durand, C. David, and H. Lee, "How does the unique space-time sampling of the SWOT Mission influence river discharge series characteristics?," *Geophys. Res. Lett.*, vol. 46, no. 14, pp. 8154–8161, 2019.
[30] C. Nickles, E. Beighley, and D. Feng, "The applicability of SWOT's non-uniform space–time sampling in hydrologic model calibration," *Remote Sens.*, vol. 12, no. 19, 2020, Art. no. 3241.
[31] A. Domeneghetti, A. Tarpanelli, L. Grimaldi, A. Brath, and G. Schumann, "Flow duration curve from satellite: Potential of a lifetime SWOT mission," *Remote Sens.*, vol. 10, no. 7, 2018, Art. no. 1107.
[32] M. W. Hagemann, C. J. Gleason, and M. T. Durand, "BAM: Bayesian AMHG-manning inference of discharge using remotely sensed stream width, slope, and height," *Water Resource Res.*, vol. 53, pp. 9692–9707, 2017.
[33] D. Feng, C. J. Gleason, and P. Lin, "Recent changes to Arctic river discharge," *Nature Commun.*, vol. 12, no. 1, 2021, Art. no. 6917.
[34] H. Guo, X. Wan, and H. Wang, "Validation of just-released SWOT L2 KaRIn beta prevalidated data based on restore the marine gravity field and its application," *IEEE J. Sel. Topics Appl. Earth Observ. Remote Sens.*, vol. 17, pp. 7878–7887, Mar. 2024.
[35] N. M. Desrochers et al., "Effects of aquatic and emergent riparian vegetation on SWOT mission capability in detecting surface water extent," *IEEE J. Sel. Topics Appl. Earth Observ. Remote Sens.*, vol. 14, pp. 12467–12478, Nov. 2021.
[36] C. Wang and S. Chen, "Ground elevation accuracy verification of ICESat-2 data: A case study in Alaska, USA," *Opt. Express*, vol. 27, no. 26, pp. 38168–38179, 2019.
[37] A. Liu, X. Cheng, and Z. Chen, "Performance evaluation of GEDI and ICESat-2 laser altimeter data for terrain and canopy height retrievals," *Remote Sens. Environ.*, vol. 264, 2021, Art. no. 112571.
[38] G. Li, J. Guo, L. Pei, S. Zhang, X. Tang, and J. Yao, "Extraction and analysis of the three-dimensional features of crevasses in the amery ice shelf based on ICESat-2 ATL06 data," *IEEE J. Sel. Topics Appl. Earth Observ. Remote Sens.*, vol. 14, pp. 5796–5806, Jun. 2021.
[39] B. Liu, X. Ma, J. Guo, and R. Wen, "Extending the wind profile beyond the surface layer by combining physical and machine learning approaches," *Atmospheric Chem. Phys.*, vol. 24, no. 7, pp. 4047–4063, 2024.
[40] D. Shailen, "Surface water and ocean topography mission (SWOT) project: Science requirements document," Jet Propulsion Lab., Pasadena, CA, USA, 2018.
[41] N. M. Desrochers et al., "Effects of aquatic and emergent riparian vegetation on SWOT mission capability in detecting surface water extent," *IEEE J. Sel. Topics Appl. Earth Observ. Remote Sens.*, vol. 14, pp. 12467–12478, Nov. 2021.
[42] C. M. Birkett, M. Ricko, B. D. Beckley, X. Yang, and R. L. Tetrault, "G-REALM: A lake/reservoir monitoring tool for drought monitoring and water resources management," in *Proc. AGU Fall Meeting*, 2017, vol. 2017, pp. H23P–H202.
[43] Z. Duan and W. G. M. Bastiaanssen, "Estimating water volume variations in lakes and reservoirs from four operational satellite altimetry databases and satellite imagery data," *Remote Sens. Environ.*, vol. 134, pp. 403–416, 2013.
[44] A. A. J. Cretaux and S. Calmant, "Recent developments in hydroweb database water level time series on lakes and reservoirs," in *Proc. AGU Fall Meeting*, 2013, vol. 2013, pp. GC23F–GC207.
[45] E. Park, "Characterizing channel-floodplain connectivity using satellite altimetry: Mechanism, hydrogeomorphic control, and sediment budget," *Remote Sens. Environ.*, vol. 243, 2020, Art. no. 111783.
[46] B. Lehner and G. Grill, "Global river hydrography and network routing: Baseline data and new approaches to study the world's large river systems," *Hydrol. Process.*, vol. 27, no. 15, pp. 2171–2186, 2013.
[47] B. Liu, X. Ma, J. Guo, R. Wen, and W. Gong, "Extending the wind profile beyond the surface layer by combining physical and machine learning approaches," *Atmospheric Chem. Phys.*, vol. 24, no. 7, pp. 4047–4063, 2024.

Linpeng Yu received the B.S. degree in information science and engineering, Shandong University, Qingdao, China.

His research interests include the study of electronic devices, communications, and part of the satellite remote sensing research.

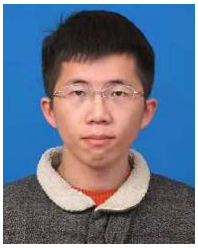

Haowei Zhang received the B.S. degree in remote sensing science and technology from the Heilongjiang Institute of Engineering, Harbin, China, in 2019, and the M.S. degree in surveying and mapping engineering in 2022 from Wuhan University, Wuhan, where he is currently working toward the Ph.D. degree in physical electronics.

His research interests include LiDAR ranging and remote sensing of environment.

Wei Gong received the B.S. degree in photonics engineering from the Huazhong University of Science and Technology (HUST), Wuhan, China, in 1993, the M.S. degree in electronics from the Chinese Academy of Science, Lanzhou, China, in 1996, and the Ph.D. degree in physical electronics from HUST, in 1999.

He was an Assistant Professor with Hampton University, Hampton, VA, USA, from 2002 to 2004. He is a Professor with the State Key Laboratory of Information Engineering in Surveying, Mapping and Remote Sensing, Wuhan University, Wuhan. His research interests inlude teaching and research of new laser, optical technology, and its remote sensing applications, and has made achievements in atmospheric LiDAR and optical remote sensing. He has authored more than 100 scientific articles, holds 18 patents, and has coauthored 2 books.

Dr. Gong was a recipient of the New Century Excellent Talents in 2007, the Luojia Scholars, the Chutian Scholars in 2010, and the Yangtze River Scholars in 2014.

Xin Ma received the the B.S., M.S., and Ph.D. degrees in photogrammetry and remote sensing from Wuhan University, Wuhan, China, in 2010, 2013, and 2016, respectively.

He is an Assistant Professor with the State Key Laboratory of Information Engineering in Surveying, Mapping and Remote Sensing, Wuhan University.